Am J Cancer Res 2024;14(3):1052-1070
www.ajcr.us /ISSN:2156-6976/ajcr0155100

Original Article

Multi-omics and tumor immune microenvironment characterization of a prognostic model based on aging-related genes in melanoma

Zhenghao He[1], Manli Chen[1], Qianwen Li[2], Zhijun Luo[1*], Xidie Li[3*]

[1]Department of Plastic Surgery, Zhongshan City People's Hospital, Zhongshan, Guangdong, China; [2]Department of Dermatology, The Second Xiangya Hospital, Central South University, Hunan Key Laboratory of Medical Epigenomics, Changsha, Hunan, China; [3]Department of Gynaecology and Obstetrics, The Affiliated Zhuzhou Hospital Xiangya Medical College, Central South University, Zhuzhou, Hunan, China. [*]Co-corresponding authors.

Received December 24, 2023; Accepted March 8, 2024; Epub March 15, 2024; Published March 30, 2024

Abstract: Melanoma is a common and fatal cutaneous malignancy with strong invasiveness and high mortality rate. Clinically, elderly melanoma patients tend to exhibit stronger invasion ability and poorer prognosis. Given the heterogeneity of tumors, we analyzed the prognosis and risk assessment of melanoma through aging-related genes rather than age stratification. FOXM1 and CCL4 were identified to be closely associated with melanoma prognosis. Single-cell transcriptome analysis showed that FOXM1 was significantly up-regulated in tumor cells, while CCL4 was markedly elevated in immune cells. A melanoma prognostic model was constructed based on the two independent prognostic factors. This model showed a high accuracy in predicting the mortality of melanoma patients over several years. The patients in low-risk group appeared to have more immune cell infiltration and better immune therapy efficacy. Cellular experiments showed that CCL4 could promote apoptosis of melanoma cells through immune cells, and apoptosis could regulate the expression of FOXM1. In addition, the results of the spatial transcriptome and immunohistochemistry suggested that CCL4 was highly expressed in macrophages and the expression of FOXM1 in melanoma cell was negatively correlated with immune cell infiltration, especially macrophages. Here, we established a novel prognostic model for melanoma, which showed promising predictive performance and may serve as a biomarker for the efficacy of immune checkpoint inhibition therapy in melanoma patients. In addition, we explored the function of two genes in the model in melanoma.

Keywords: Aging-related genes, prognostic model, melanoma, tumor immune microenvironment

Introduction

Melanoma is a highly lethal tumor that occurs in 5% of total skin malignancies, yet melanoma patients account for more than 75% of deaths from skin malignancies [1]. The incidence of melanoma has increased rapidly over the past 30 years. According to U.S. cancer statistics, approximately 76,000 people were diagnosed with melanoma in 2017 in the United States [2]. The global annual death toll from melanoma is as high as 55,500 [3]. In addition, 20%~30% of melanoma originates in mucous membranes, such as vulvar melanoma, oral melanoma, and choroid melanoma [4-7]. Therefore, melanoma is a multidisciplinary concerned disease because of the hidden symptoms at the initial stage, which make its diagnostic prickly for gynecologist, ophthalmologists, etc. Although many advances have been made in new adjuvant immunotherapy, chemotherapy, and targeted therapy for melanoma in recent years, the treatment of advanced malignant melanoma remains a daunting challenge for clinicians.

The risk prediction models used to define high-risk populations of disease have been widely applied in clinical practice. Early diagnosis, accurate assessment, and timely intervention are crucial for reducing the mortality rate of melanoma patients and improving their prognosis [8]. Traditional prognostic models are mostly based on patient age, gender, clinical features, histopathological changes, etc. However, the individual heterogeneity, complex pathological

https://doi.org/10.62347/UZGP9704

classification, and unclear pathogenesis of malignant melanoma lead to a difficult prognostic assessment of melanoma. With the booming development of sequencing and bioinformatics analysis technologies in recent years, models based on gene expression features for risk evaluation of melanoma patients have gradually attracted attention.

The middle-aged and elderly population is easily affected by melanoma. Epidemiological studies have shown that the prognosis of elderly patients is far worse than that of young patients. Age, or aging, is considered the biggest risk factor for cancer development. Aging provides time for precancerous cells to accumulate mutations, and the increase of age-related senescence-associated secretory phenotype (SASP) can promote the development of melanoma. A recent study showed that the arrangement of extracellular matrix in the skin of older patients can make melanoma cells more invasive [9, 10]. Although there is clearly a correlation between aging and lifespan, age is not an ideal indicator for prognostic risk assessment of melanoma given the complex heterogeneity of individual tissue aging. Therefore, in this study, we attempted to evaluate the prognosis and risk of melanoma from the perspective of aging-related genes, with the aim of providing new ideas for the construction of a prognostic assessment model for melanoma.

In this study, we downloaded a dataset of melanoma patients from the TCGA database and an aging-related gene set from the AgingAtlas database. By the COX analysis and LASSO analysis, we identified FOXM1 and CCL4 as two aging-related genes highly correlated with melanoma prognosis. Then we successfully established a melanoma aging-related prognostic model that could better reflect mortality and treatment response rates. Finally, we confirmed the relationship between these two gene expressions and melanoma development at the single-cell level, spatial transcriptome, and immunohistochemical level.

Methods

Genes and patients

We downloaded 499 aging-related genes from AgingAtlas (https://ngdc.cncb.ac.cn/aging/index) [11]. The melanoma-related sequencing data from TCGA came from the Xena database (https://xena.ucsc.edu/) and were filtered based on the availability of survival data [12]. Other melanoma datasets are from the GEO database, details can be found in the Patient characteristics (**Table 1**).

Survival analysis

Based on the expression levels of aging-related genes and patient survival information, we used univariate Cox analysis to identify genes associated with melanoma prognosis. We further focused on key genes through Lasso analysis and multivariate Cox analysis.

Single cell sequencing and spatial transcriptome sequencing analysis

The melanoma single-cell transcriptome dataset GSE115978 was downloaded from the GEO database (CreateSeuratObject: min.cells = 5, min.genes = 2000), the dataset was normalized with principal component analysis (PCA) [13]. The dim was set to 20 according to the ElbowPlot results, and the data was analyzed by dimensionality reduction using UMAP, and finally, each cluster was annotated. The melanoma spatial transcriptome dataset was downloaded using the BayesSpace package, and the dataset was clustered through the spatialCluster (q=4, d=10, nrep = 1000, burn.in = 10, init.method = 'mclust', model = 't') and spatialEnhance (q=4, d=5, nrep = 1000, burn.in = 10, model = 't') functions, and each cell cluster was annotated according to biomarkers [14].

Establish a melanoma prognostic model

A melanoma prognostic model was established based on multivariate Cox analysis, and the risk score of each patient was calculated according to the model. Time-dependent ROC was used to evaluate the predictive ability of the model for patient survival. The prognostic effect of the model was validated in the GSE19234 and GSE65904 datasets [15, 16]. In addition, the predictive effect of the model on the efficacy of immunotherapy in melanoma patients was explored.

Multi-omics analysis

Data related to mutations, mRNA, methylation and miRNA were downloaded from Xena and patients were classified into high-risk and low-

Table 1. Patient characteristics

Datasets	Characteristic	N	Median	Standard deviation
TCGA-SKCM	Age	455	57.75	15.45
	Sex, n			
	Female	171		
	Male	284		
	Status, n			
	Alive	235		
	Dead	219		
	Not reported	1		
	Stage, n			
	0	6		
	I	77		
	II	134		
	I/II nos	10		
	III	170		
	IV	23		
	Not reported	35		
GSE115978	Age	33	67.58	12.3
	Sex, n			
	Female	10		
	Male	23		
GSE19234	Age	44	63.32	18.24
	Sex, n			
	Female	16		
	Male	28		
	Status, n			
	Alive	20		
	Dead	24		
	Stage, n			
	III	39		
	IV	5		
GSE65904	Age	214	62.35	14.4
	Sex, n			
	Female	89		
	Male	124		
	Unknown	1		
	Status, n			
	Alive	108		
	Dead	102		
	Unknown	4		

risk groups based on the prognostic model. The "maftool" package was used to analyze and visualize gene mutation data [17]. The mRNA (|logFC| > 0.7, P < 0.05) and miRNA (|logFC| > 0.7, P < 0.05) data were differentially expressed using the "limma" and "edgeR" package, and targeting relationships between mRNA-miRNAs were constructed based on the ceRNA hypothesis and the miRWalk database [18-20]. Methylation data were analyzed using a "ChAMP" package [21]. Enrichment analysis of related genes was performed using the "clusterProfiler" package [22].

Immune infiltration analysis

ESTIMATE is a tool for the assessment of tumor immune infiltration, its full name is Estimation of STromal and Immune cells in MAlignant Tumor tissues using Expression data [23]. It is a computational tool based on gene expression data, which estimates the relative proportions of tumor cells, immune cells, and stromal components in tumor tissue by analyzing gene expression data in tumor tissue. CIBERSORT is a bioinformatics method for analyzing transcriptome sequencing data [24]. It is capable of separating the expression profiles of different immune cell types from transcriptome data and thus inferring the relative abundance of each cell type. TIDE (Tumor Immune Dysfunction and Exclusion) is a bioinformatics method used to analyze tumor immunotherapy responses [25]. Its main function is to predict the response of tumor patients to immunotherapy by calculating the interaction pattern between tumor cells and immune cells. Molecular Functional Portrait (MFP) was used to analyze the malignancy of tumors and identify different tumor microenvironments, which can classify the tumor microenvironment into four different subtypes [26]. Here, we used ESTIMATE, CIBERSORT, TIDE, and MFP to analyze the immune invasion, as well as the effects on treatment and prognosis of patients in high- and low-risk groups.

Multi-immunohistochemistry staining

Firstly, high-pressure acidic antigen retrieval was performed (place the paraffin section of melanoma patients into a container containing 1× citric acid antigen repair solution (PH6.0), then put this container into the special pres-

sure cooker for experimental immunohistochemistry, adjust the power to 1000 W, and time it for 7 min). Subsequently, the slides were treated with 5% BSA and stained immunohistochemically with: CD8 (clone MX117, MXB), FCGR1A (R24290, ZEN-BIOSCIENCE), CCL4 (710391, Abcam), FOXM1 (ab207298, Abcam). The tyramide amplification kits (PerkinElmer) were used for multi-immunohistochemistry staining. The staining residues were captured by the PerkinElmer Vectra multispectral imaging system (PerkinElmer), and analyzed by inForm 2.3.1 (PerkinElmer).

Cell culture

Human melanoma cell A2058 (Abiowell) was cultured in high-glucose DMEM (gibco) containing 10% fetal bovine serum (EXcell) and 1% penicillin-streptomycin (Servicebio) and maintained in a 5% CO_2, 37°C incubator. There are four groups in the CCL4 (PeproTech) stimulation experiment: A2058, PBMC+A2058, CCL4+A2058, PBMC+CCL4+A2058, and each group has 6 samples. The UVB irradiation experiment was divided into two groups: blank control, and UVB irradiation, and each group has 12 samples.

UVB irradiation

According to the literature, the apoptosis model of melanoma cell was constructed by UVB irradiation. The specific method was to irradiate A2058 with UVB (1.5 uW/cm^2, 100 s) and observe the state of its cells after 24 hours.

Apoptosis assay

CCL4 stimulation: Peripheral blood mononuclear cells (PBMCs) were obtained from healthy volunteers and separated by lymphocyte separation medium Ficoll and density gradient centrifugation. According to the subgroups, PBMC (1.5 * 10^6 cells/well) and A2058 cells were inoculated into 24-well plates and left for 24 h. DPBS (Servicebio) was washed twice, and cells were harvested after digestion with EDTA-free trypsin (gibco) to prepare cell suspensions.

UVB irradiation: According to the grouping, A2058 was inoculated into a 12-well plate and adhered to the wall. UVB irradiation was carried out at 1.5 μW/cm^2 for 100 s. After 24 hours, cells were collected and prepared into a cell suspension.

Apoptosis cells were stained using the AnnexinV-FITC/PI Apoptosis Detection Kit (YEASEN), detected by multicolor flow cytometry (BD), and then analyzed by Flowjo software (10.7.1).

RT-qpcr

Total RNA was isolated from the cells using Trizol and reverse transcribed into cDNA using the Evo M-MLV Reverse Transcription Kit (AG Accurate Biology), and RT-qPCR was performed by the SYBR Green qPCR Kit (AG Accurate Biology) and designed primers (Forward sequence: ATACGTGGATTGAGGACCACT; Reverse sequence: TCCAATGTCAAGTAGCGGTTG) using a fluorescent quantitative PCR instrument (Bio-Rad). The 2-ΔΔCT method was utilized to measure the relative mRNA expression of FOXM1.

Cell proliferation assay

Cell proliferation was valued by the Cell Counting Kit-8 (CCK-8) Assay Kit (Servicebio). 10 μl of CCK-8 reagent was added to each well and incubated in a cell culture incubator at 5% CO_2, 37°C for 100 min. Absorbance at 450 nm was measured using an enzyme meter.

Wound healing

Cells were scraped using a 20 μl sterile plastic pipette tip and washed 3 times with DPBS to remove cell debris. 1000 μl of serum-free medium was added and incubated in a cell culture incubator at 5% CO_2, 37°C. The scratched area was imaged at 0 h, 24 h, 48 h and 72 h and measured using Imagej software (1.4.3).

Bioinformatics and statistical analysis

The bioinformatics analyses conducted within this study were all performed using R (4.2.2). To compare the mean between two conditions, a Student's t-test was used. $P < 0.05$ was considered statistically significant. The statistical significance is shown as *$P < 0.05$; **$P < 0.01$; ***$P < 0.001$ vs. control. The codes for screening key genes are shown in Supplementary Table 2.

Results

The key prognostic genes for melanoma: CCL4 and FOXM1

To identify the relationship between prognosis of melanoma and aging, we analyzed the phenotype data of melanoma patients in TCGA and found that, consistent with previous studies, the likelihood of death increased with age (Supplementary Figure 1).

However, the age of onset showed significant heterogeneity and was not an ideal indicator for evaluating prognosis. To address this issue, this study analyzed and evaluated the prognosis of melanoma from the perspective of aging-related genes. Through univariate COX analysis, we obtained 127 genes associated with prognosis in melanoma patients (The top 40 can be found in Supplementary Table 1), of which 97 genes were associated with good prognosis and 30 genes were associated with poor prognosis. By LASSO regression analysis, the number of key genes were further narrowed down to 5 (Supplementary Figure 2), namely CCL4, CREBBP, FOXM1, PARP1, and TNF. Finally, FOXM1 and CCL4 were identified as independent prognostic factors for melanoma patients by using multivariate Cox analysis (**Figure 1A**). Our results showed that melanoma patients with a better prognosis exhibited significantly higher CCL4 expression and a lower FOXM1 level than those with a worse prognosis (**Figure 1B**, **1C**).

The heterogeneity among different cell subtypes in melanoma can be well revealed by the single-cell transcriptome analysis. Therefore, we explored the expression differences of FOXM1 and CCL4 at single-cell levels in melanoma. Through PCA and UMAP dimensionality reduction analysis, the dataset containing 2977 cells from GSE115978 was classified into 13 clusters and further annotated as 8 cell subtypes (**Figure 1D**, **1E**). FOXM1 was significantly upregulated in tumor cells (Malignant) and cancer-associated fibroblast (CAF), while CCL4 was significantly upregulated in tumor immune infiltrating cells like T cells, NK cells and macrophages (**Figure 1F**). These results corroborated with the previous results of transcriptome sequencing analysis, indicating that FOXM1 was highly expressed in melanoma cells and played a pro-cancer role, while CCL4 was highly expressed in immune cells and played an anti-cancer role.

Construction of melanoma prognostic model by the CCL4 and FOXM1

An ideal prognostic model of a tumor is one that can give hints on the patient's risk of future death and response to treatment. Combined the two key prognostic genes for melanoma (CCL4 and FOXM1), we established a melanoma prognostic model by multifactorial COX analysis: risk score of melanoma = (-0.25484 * CCL4) + (0.26607 * FOXM1). Based on this model, the risk score of each patient was calculated and ranked from smallest to largest, and it was found that as the risk score increased, the likelihood of patient death also increases (**Figure 2A-C**). In addition, we analyzed the effectiveness of this model by the time-dependent ROC analysis. At 12, 24, 36, 48, and 60 months, the area under the curve was 0.7, 0.7, 0.67, 0.65, and 0.65, respectively (**Figure 3A**), supporting the high accuracy of this prognostic model in predicting the mortality of melanoma patients over several years.

Furthermore, we validated the model using the GSE19234 and GSE65904 datasets, and as expected, the prognosis of patients in the low-risk group was better (**Figure 3B**, **3C**). To verify the validity of the model for immunotherapy prediction, we analyzed the GSE35640 dataset. Patients with effective or ineffective immune checkpoint inhibition therapy were grouped according to their risk scores, and significant improvements in the efficacy of immunotherapy were found in the low-risk group through chi-square analysis (**Figure 3D**).

The analysis of multi-omics in high-risk and low-risk groups of melanoma

To further confirm the classification significance of this melanoma prognostic model, more differences between high-risk and low-risk populations were analyzed by the analysis of multi-omics. Based on the risk score, melanoma patients were divided into high-risk and low-risk groups, and differences in the mutations of genes, the expression of mRNA, methylation and miRNA between the two groups were analyzed in detail.

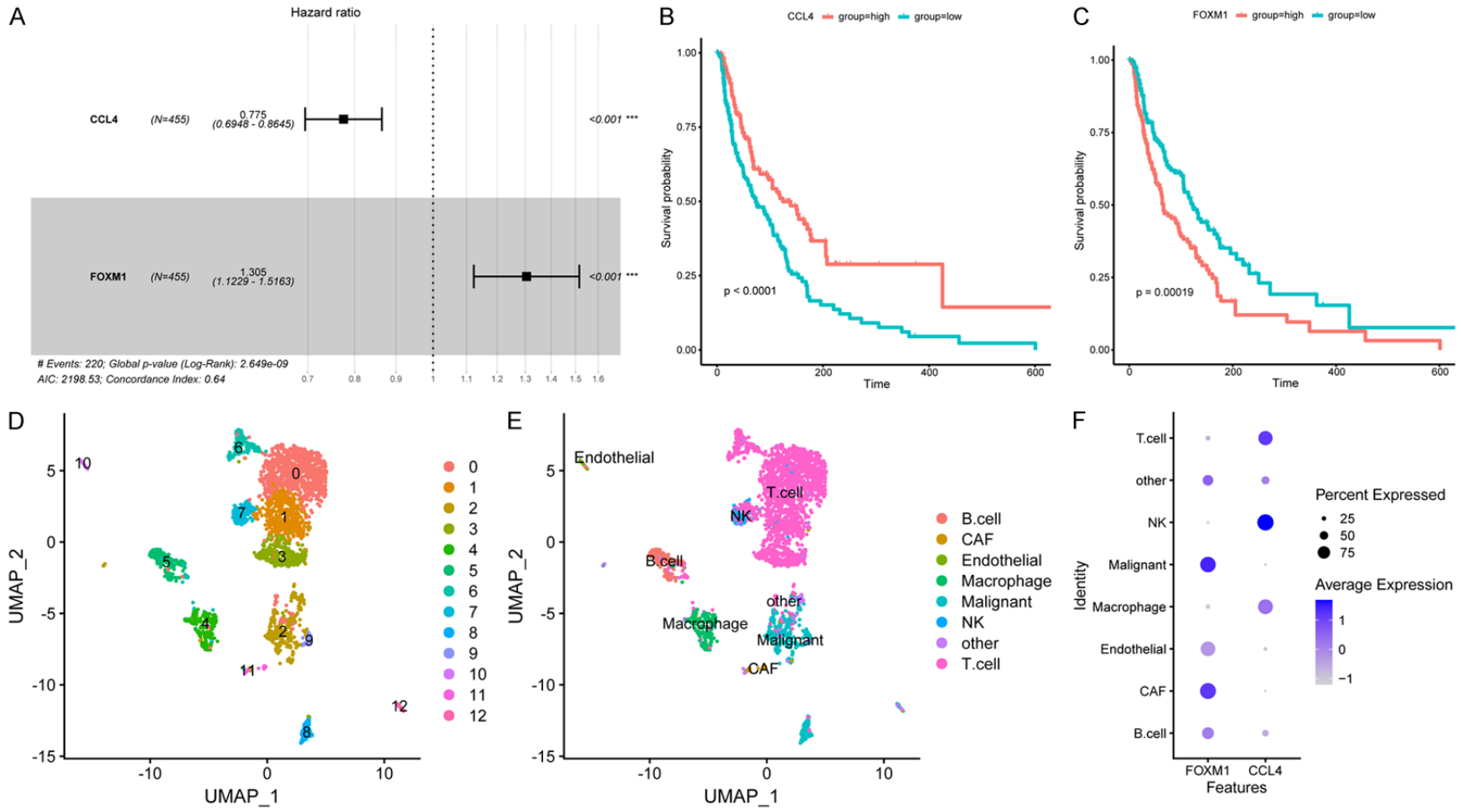

Figure 1. The expression of CCL4 and FOXM1 is closely related to the prognosis of melanoma patients and has cell heterogeneity in tumor tissues. (A) As the Random forest plot shown, CCL4 and FOXM1 were independent factors for the prognosis of melanoma patients. (B) The survival analysis of melanoma patients based on the expression of CCL4. (C) The survival analysis of melanoma patients based on the expression of FOXM1. (D) 2977 cells from GSE115978 were classified into 13 clusters by the UMAP analysis. (E) 8 subtypes obtained from the cell clusters in (D) by the cell annotation. (F) Expression levels of FOXM1 and CCL4 in 8 subtypes of cells.

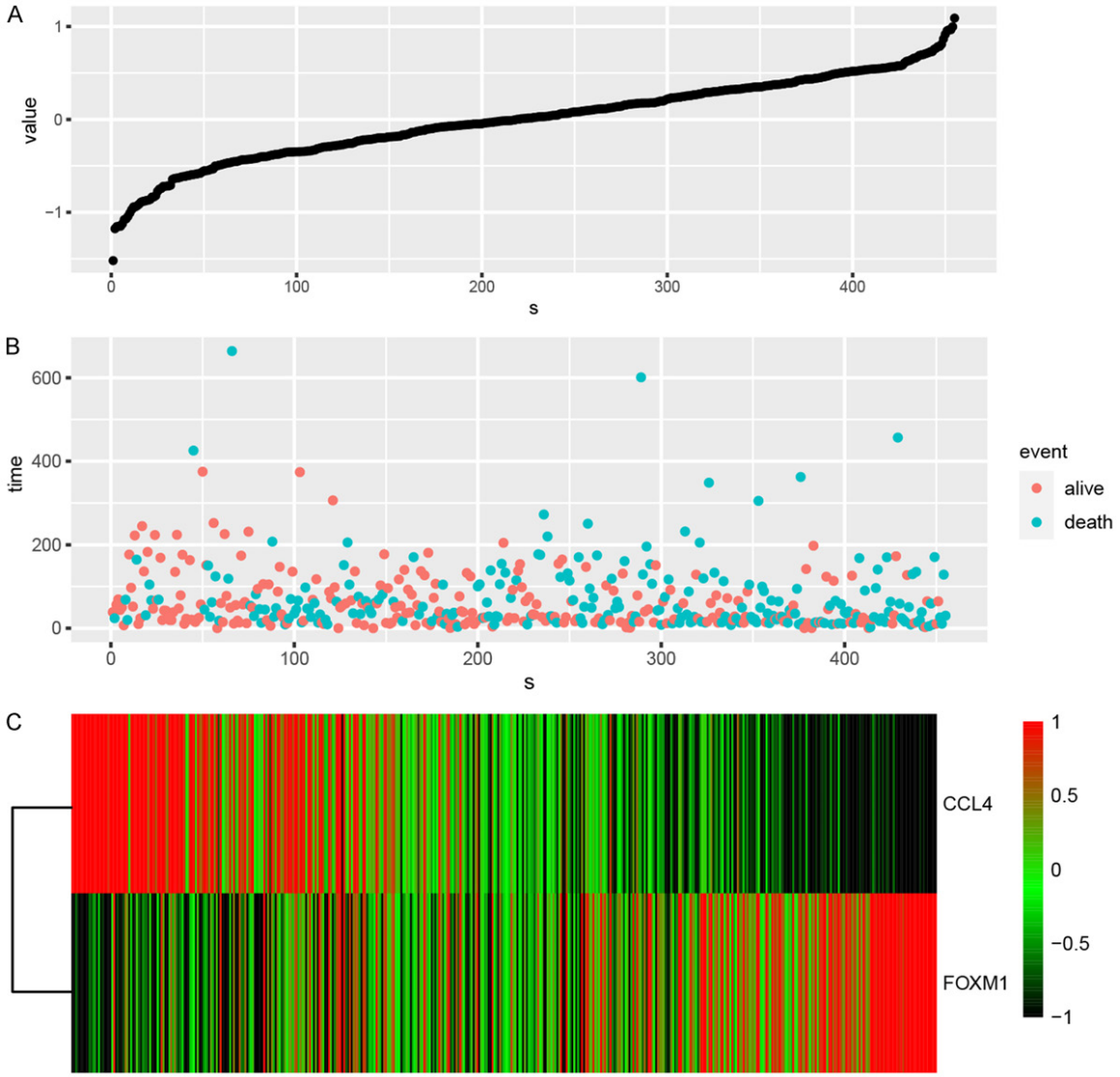

Figure 2. Construction of melanoma prognostic model by the CCL4 and FOXM1. A. The melanoma patients were scored based on our melanoma prognostic model and sorted in ascending order. The horizontal axis represents each patient, and the vertical axis represents the corresponding risk score. B. Patients were also arranged according to their risk scores and labeled with their follow-up duration. The horizontal axis represents each patient, and the vertical axis represents the duration of follow-up. Red represents patients in a survival state, and blue represents patients who have died. It can be observed that high-risk patients have more blue dots and shorter follow-up duration. C. Heatmap of CCL4 and FOXM1 expression in melanoma patients. Red represents high expression, and black represents low expression. It can be found that CCL4 is highly expressed in low-risk patients, while FOXM1 is highly expressed in high-risk patients.

The higher the Variant Allele Frequency (VAF), the higher the tumor heterogeneity and the tumor purity are. In the high-risk group, it was obviously seen that the VAF of the most mutated genes was significantly higher than that of the low-risk group (**Figure 4A**, **4B**). Kataegis is defined as a genomic fragment comprising six or more consecutive mutations with an average mutation spacing of less than or equal to 100 bp. TCGA-FW-A3R5 is an example of a sample in the high-risk group, while TCGA-EE-A2MR is an example of a sample in the low-risk group. It is evident that TCGA-FW-A3R5 has more C > T mutations and more Kataegis as compared to TCGA-EE-A2MR (**Figure 4C**, **4D**). In the comparison of gene mutations between the high- and

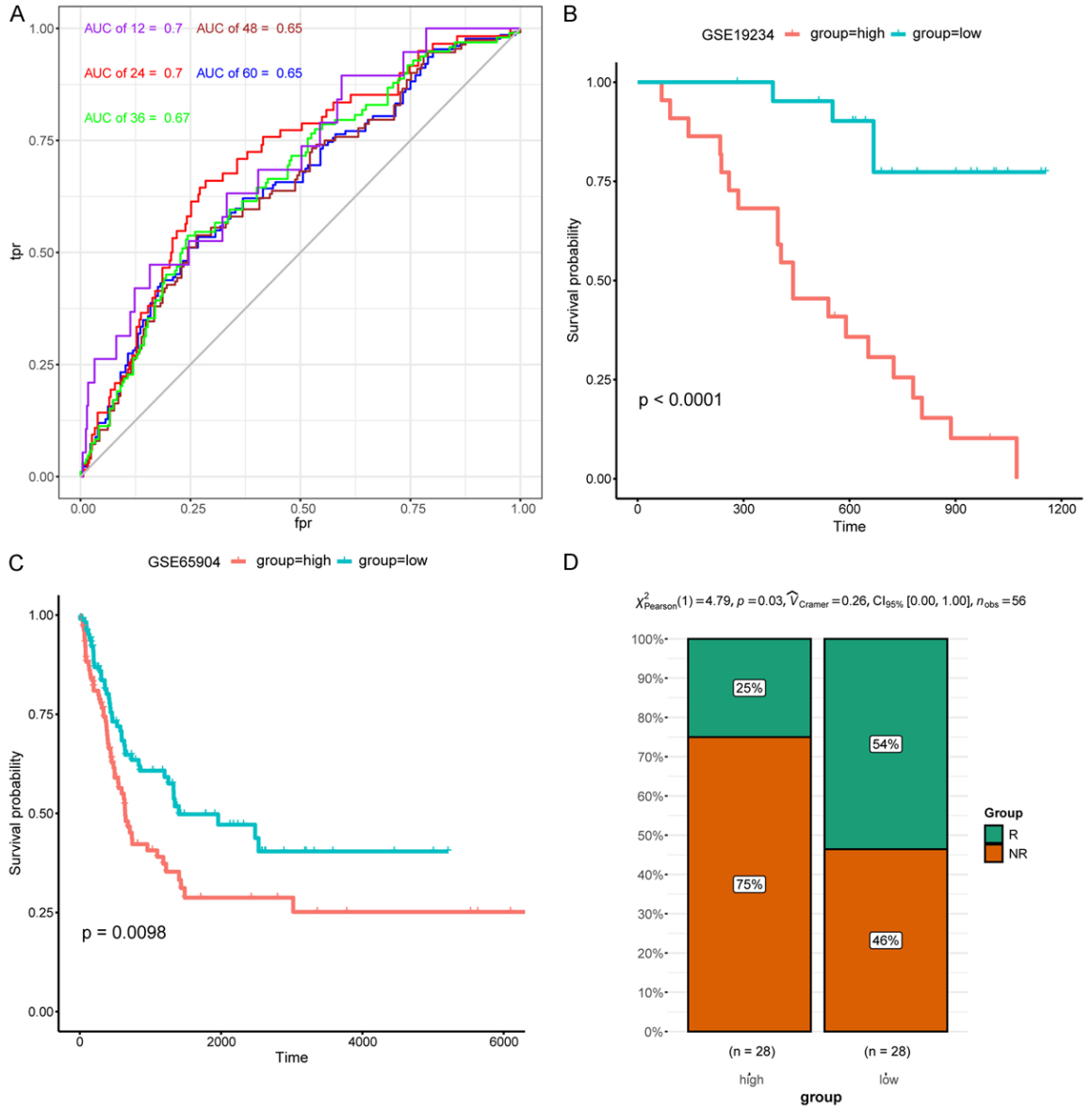

Figure 3. Validate the ability of the model to predict prognosis and immunotherapy response in melanoma patients. A. ROC analysis showd the effectiveness of our model in predicting prognosis in melanoma patients at 12, 24, 36, 48, and 60 months. B. The effectiveness of the model was validated in the GSE19234 dataset, where red represents the high-risk group and blue represents the low-risk group. It is obvious that patients in the high-risk group have a worse prognosis. C. The validity of the model was verified in the GSE65904, and patients in the high-risk group had worse prognosis. D. Patients in the GSE35640 were divided into high- and low-risk groups according to the model, and chi-square test revealed that patients in the low-risk group had a higher effective rate of immune checkpoint inhibition therapy.

low-risk groups, we found more specific mutated genes in the high risk group, including BCL2L12, OGDH, etc. (**Figure 5A**).

Compared with low-risk group patients, high-risk group patients showed higher expression of mRNA and lower methylation of genes related to "AMPK signaling pathway", whereas lower expression of mRNA and higher methylation levels of genes related to the "MAPK signaling pathway", "PD-L1 expression and PD-1 checkpoint pathway in cancer", "Natural killer cell mediated cytotoxicity", "Chemokine signaling pathway" and "Cytokine-cytokine receptor in-

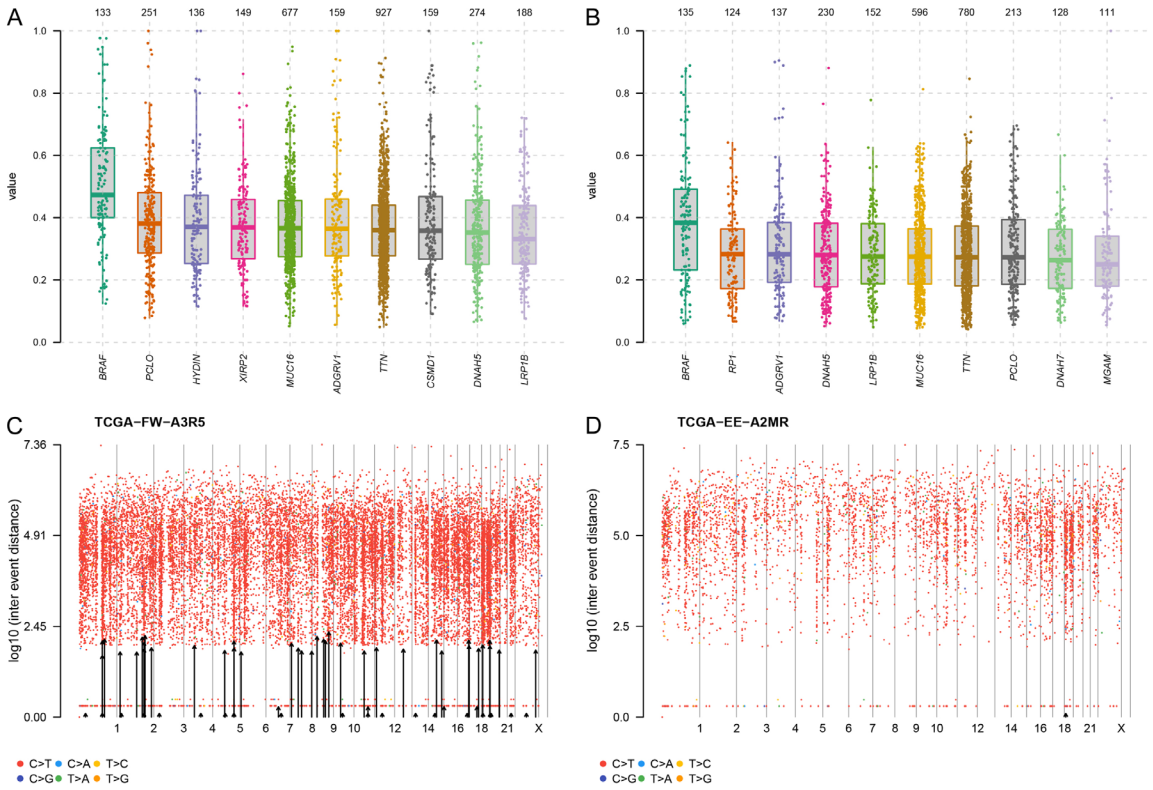

Figure 4. Differences in gene mutation levels between high- and low-risk groups. (A, B) As the VAF increases, tumor heterogeneity and purity also increase. It can be clearly seen that the VAF in the high-risk group represented by the (A) is significantly higher than that in the low-risk group represented by the (B). (C, D) Each arrow represents a Kataegis. It can be clearly seen that the samples representing the high-risk group in the (C) have more C > T mutations and more Kataegis than the samples representing the low-risk group in the (D).

teraction" (**Figure 5B**). These pathways have been reported to play important roles in the pathogenesis of melanoma in previous studies.

According to the ceRNA hypothesis, a targeting relationship between these differentially expressed mRNAs and miRNAs was found in our results (**Figure 5C**). All of the mRNAs in the **Figure 5C** were poorly expressed in the high-risk group of patients, and all miRNAs associated with these mRNAs were highly expressed. We conducted enrichment analysis on these mRNAs and found that they were mainly enriched in signaling pathways such as "humoral immune response" and "positive regulation of T cell activation" (**Figure 5D**), indicating that the differential gene between high-risk and low-risk group patients are epigenetically regulated and closely related to the immune response.

In addition, our analysis of GSE115978 also revealed that risk scores were higher in Malignant and CAF cell subpopulations and lower in immune cells (**Figure 5E**). Interestingly, risk scores also declined to some extent in patients with melanoma after treatment as compared to before treatment (**Figure 5F**). This result demonstrated that our model not only had a certain effect at the tissue level, but also at the cellular level.

Correlation analysis between melanoma risk score and tumor immunity

The above multi-omics analyses have suggested that risk scores are closely related to tumor immunity. So we explored this further by using ESTIMATE, TIDE and CIBERSORT. In the ESTIMATE analysis, patients in the high-risk group were found to have lower StromalScore, ImmuneScore and ESTIMATEScore scores and higher TumorPurity than patients in the low-risk group, which was consistent with the results obtained in the analysis of VAF (**Figure 6A-D**). The ESTIMATE analysis results showed that in

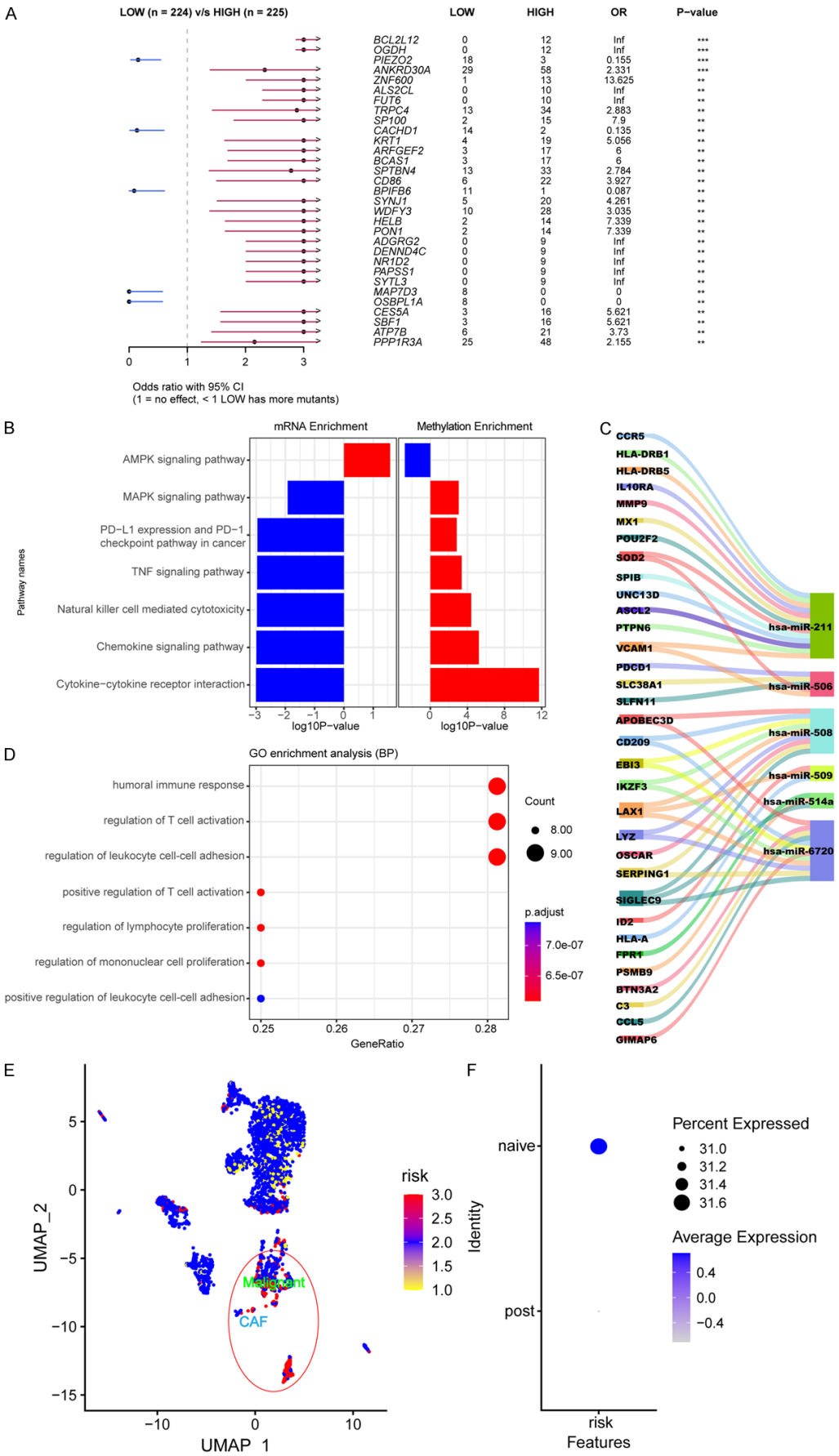
A
LOW (n = 224) v/s HIGH (n = 225)
LOW
HIGH
OR
P−value
BCL2L12 0 12 Inf ***
OGDH 0 12 Inf ***
PIEZO2 18 3 0.155 ***
ANKRD30A 29 58 2.331 ***
ZNF600 1 13 13.625 **
ALS2CL 0 10 Inf **
FUT6 0 10 Inf **
TRPC4 13 34 2.883 **
SP100 2 15 7.9 **
CACHD1 14 2 0.135 **
KRT1 4 19 5.056 **
ARFGEF2 3 17 6 **
BCAS1 3 17 6 **
SPTBN4 13 33 2.784 **
CD86 6 22 3.927 **
BPIFB6 11 1 0.087 **
SYNJ1 5 20 4.261 **
WDFY3 10 28 3.035 **
HELB 2 14 7.339 **
PON1 2 14 7.339 **
ADGRG2 0 9 Inf **
DENND4C 0 9 Inf **
NR1D2 0 9 Inf **
PAPSS1 0 9 Inf **
SYTL3 0 9 Inf **
MAP7D3 8 0 0 **
OSBPL1A 8 0 0 **
CES5A 3 16 5.621 **
SBF1 3 16 5.621 **
ATP7B 6 21 3.73 **
PPP1R3A 25 48 2.155 **
0 1 2 3
Odds ratio with 95% CI
(1 = no effect, < 1 LOW has more mutants)
B
mRNA Enrichment
Methylation Enrichment
Pathway names
AMPK signaling pathway
MAPK signaling pathway
PD−L1 expression and PD−1 checkpoint pathway in cancer
TNF signaling pathway
Natural killer cell mediated cytotoxicity
Chemokine signaling pathway
Cytokine−cytokine receptor interaction
−3 −2 −1 0 1
log10P−value
0 4 8 12
log10P−value
C
CCR5
HLA-DRB1
HLA-DRB5
IL10RA
MMP9
MX1
POU2F2
SOD2
SPIB
UNC13D
ASCL2
PTPN6
VCAM1
PDCD1
SLC38A1
SLFN11
APOBEC3D
CD209
EBI3
IKZF3
LAX1
LYZ
OSCAR
SERPING1
SIGLEC9
ID2
HLA-A
FPR1
PSMB9
BTN3A2
C3
CCL5
GIMAP6
hsa-miR-211
hsa-miR-506
hsa-miR-508
hsa-miR-509
hsa-miR-514a
hsa-miR-6720
D
GO enrichment analysis (BP)
humoral immune response
regulation of T cell activation
regulation of leukocyte cell-cell adhesion
positive regulation of T cell activation
regulation of lymphocyte proliferation
regulation of mononuclear cell proliferation
positive regulation of leukocyte cell-cell adhesion
0.25 0.26 0.27 0.28
GeneRatio
Count
8.00
9.00
p.adjust
7.0e-07
6.5e-07
E
UMAP_2
UMAP_1
5 0 −5 −10 −15
−10 0 10
Malignant
CAF
risk
3.0
2.5
2.0
1.5
1.0
F
naive
post
Identity
risk
Features
Percent Expressed
31.0
31.2
31.4
31.6
Average Expression
0.4
0.0
−0.4

Figure 5. The analysis of multi-omics in high-risk and low-risk groups of melanoma. (A) As the forestplot shown, there are more specific mutated genes in the high-risk group of patients. (B) Highly expressed genes and hypomethylated genes in the high-risk group are enriched in the "AMPK signaling pathway", while low-expressed genes and hypermethylated genes are enriched in the "MAPK signaling pathway", etc. (C) Targeting relationships between low-expressed mRNA and high-expressed miRNA were found in the high-risk group according to the ceRNA hypothesis. (D) Enrichment analysis of miRNA-regulated mRNA in the (C) revealed that they are mainly related to immune pathways. (E) The total cells from GSE115978 were scored based on our melanoma prognostic model. It was found that high-risk cells are mainly malignant and CAF cells. (F) After treatment in patients with melanoma, the risk score also significantly decreased.

the low-risk group of patients, there were more immune cells and stromal cells, and the malignancy of the tumor was relatively lower. Compared to the high-risk group, patients in the low-risk group often have a better prognosis. In the TIDE analysis, we found that the CTL scores and CD274 scores were higher in the low-risk group than in the high-risk group, suggesting that there was more cytotoxic T lymphocyte (CTL) infiltration in the low-risk group and that the efficacy of immunotherapy checkpoint suppression therapy might be better (**Figure 6E**, **6F**). In the CIBERSORT analysis, we found that the proportions of Plasma cells, CD8 T cells, activated CD4 memory T cells, Tregs, activated NK cells, Monocytes, and Macrophages M1 were higher in the low-risk group patients than in the high-risk group, while the proportions of resting CD4 memory T cells, Macrophages M0, Macrophages M2, and resting Mast cells were higher in the high-risk group than in the low-risk group (**Figure 6G**). This is mutually corroborated with the previous results, and the risk score is closely related to immune cell infiltration. The lower the score, the more immune cell infiltration in the tumor microenvironment, and the better the prognosis may be.

We used MFP analysis to classify melanoma into four subtypes: immune-enriched, non-fibrotic (IE); immune-enriched, fibrotic (IE/F); fibrotic (F); and immune-depleted (D). It is widely known that the tumor microenvironment can affect patients' response to clinical outcomes and treatment. Typically, the subtypes of IE and IF/F have more antitumor immunity and may benefit more from immune checkpoint inhibition therapy. In the TCGA melanoma dataset, the D group had the highest risk score of melanoma, followed by the F group, and the IE and IE/F groups had the lowest scores, with no significant difference between the two groups (**Figure 6H**). Similar results can be seen in the GSE22153 dataset (**Figure 6I**). These results demonstrate that our melanoma prognostic model can reflect the tumor microenvironment and predict the efficacy of immune checkpoint inhibition therapy.

Immune infiltration is closely related to tumor development, and in this study, we analyzed the relationship between the risk model and immune infiltration as well as melanoma from multiple perspectives using a variety of immune infiltration analysis methods. The results showed that patients in the low-risk group had better immune infiltration than patients in the high-risk group. Therefore, consistent with the previous analysis, the treatment response and prognosis of low-risk group patients are better than those of high-risk group patients.

CCL4 and FOXM1 are associated with apoptosis in melanoma

Flow cytometry results indicated that the co-culture of CCL4 and PBMC (P+C) with melanoma cells significantly increased the apoptosis rate of melanoma cells compared to the NC group (melanoma cells), C group (melanoma cells + CCL4), and P group (melanoma cells + PBMC) (6 samples per group) (**Figure 7A**). Meanwhile, the results of CCK-8 also suggested that the cell proliferation ability of melanoma cells in the P+C group was significantly lower than the other three groups (**Figure 7B**). Therefore, we speculated that CCL4 could induce apoptosis of melanoma cells by stimulating immune cells and reducing the malignancy of melanoma. According to the literature, we established an apoptosis model of melanoma cells using UVB irradiation demonstrated the validity of the model by detecting the percentage of melanoma cell apoptosis using flow cytometry (12 samples per group) (**Figure 7C-E**) [27]. RT-qPCR results showed a significant decrease in the expression of FOXM1 in the apoptosis group, suggesting that FOXM1 may be associated with apoptosis (**Figure 7F**). In addition, the results of CCK-8 and wound heal-

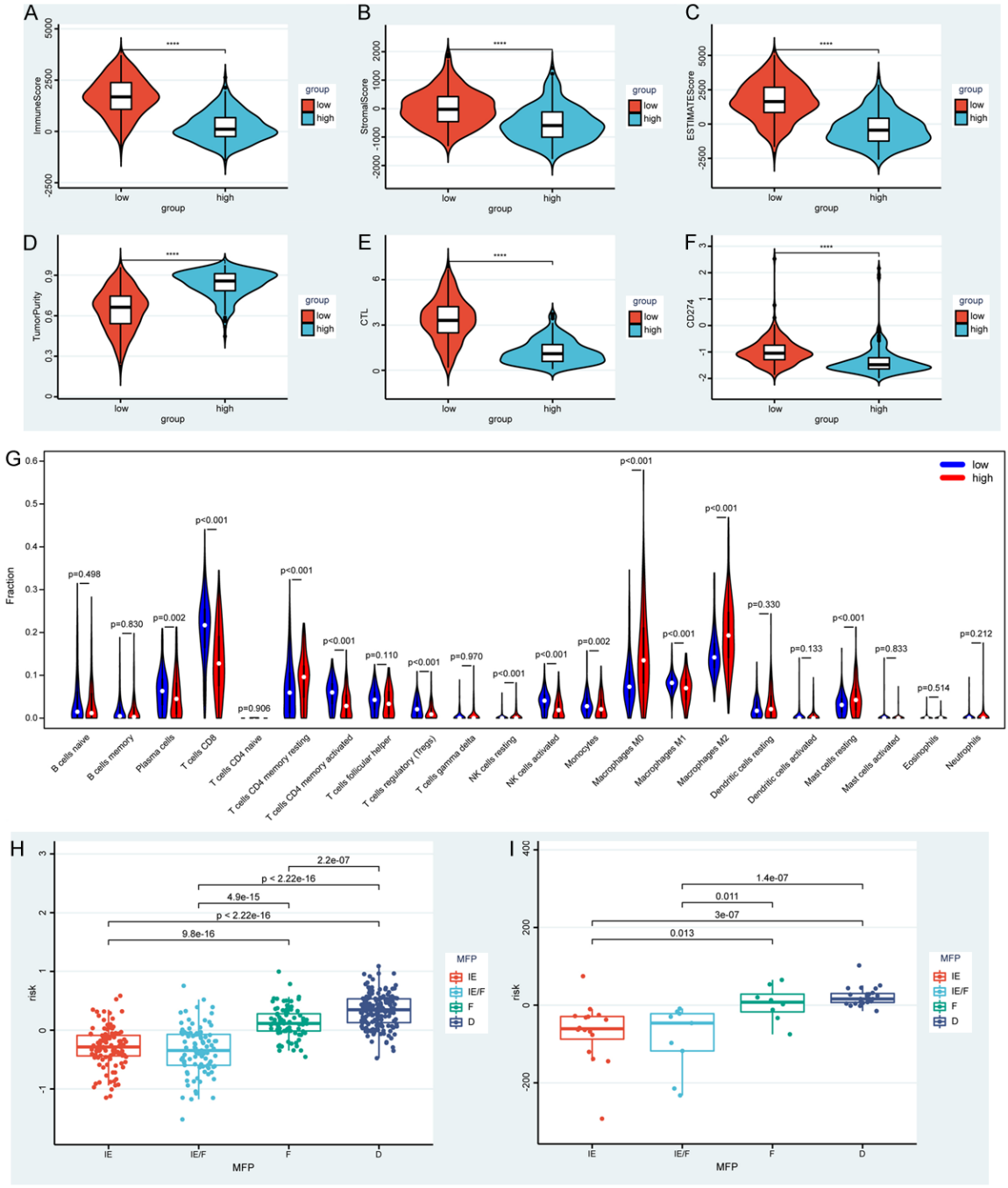

Figure 6. Correlation between prognosis model and immune infiltration of melanoma. (A-D) The comparison of ImmuneScore (A); StromalScore (B); ESTIMATEScore (C); TumorPurity (D) between high- and low-risk group patients by ESTIMATE analysis. (E, F) The comparison of CTL Score (E); CD274 Score (F) between high- and low-risk group patients by TIDE analysis. (G) CIBERSORT analysis of high- and low-risk group patients revealed significant increases in Plasma cells, CD8 T cells, activated CD4 memory T cells, Tregs, activated NK cells, Monocytes, and Macrophages M1 in the low-risk group. (H) By MFP analysis, melanoma patients from TCGA were divided into four subtypes: immune-enriched, non-fibrotic (IE); immune-enriched, fibrotic (IE/F); fibrotic (F); and immune-depleted (D). Then we compared the risk score of these four subtypes. (I) The comparison of the risk scores of four subtypes classified by MFP analysis in the GSE22153 dataset. ****denotes *P* value < 0.0001.

ing suggested that the proliferation and migration capacity of melanoma cells in the apoptotic group is reduced (**Figure 7G-I**). These results suggested that CCL4 might regulate the proliferation of melanoma cells by stimulating immune cells, and apoptosis could reduce the

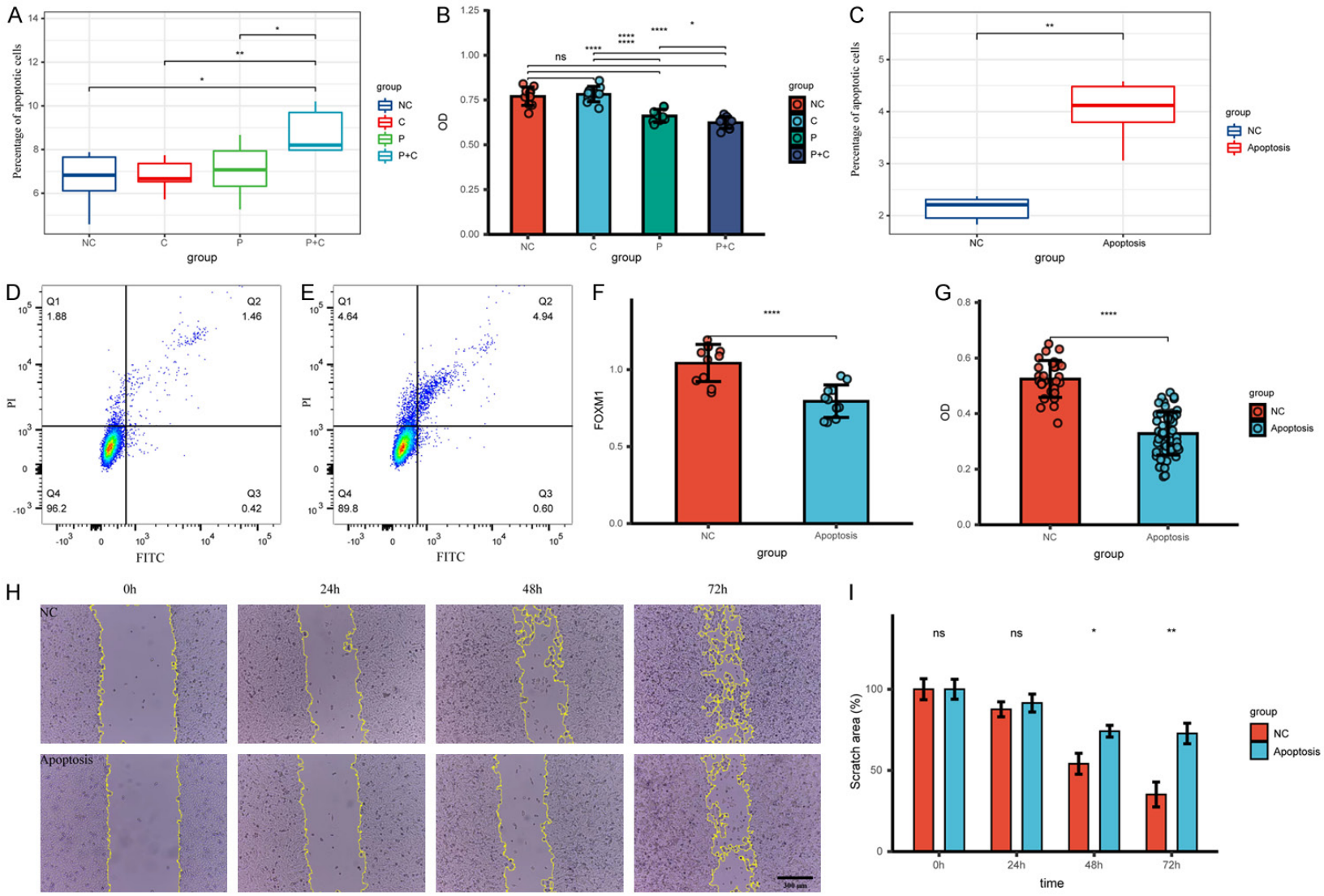

Figure 7. CCL4 and FOXM1 are associated with apoptosis in melanoma. A. Apoptosis ratio of melanoma cells in the NC, C, P and P+C groups (n=6). B. The OD value of melanoma cells in the NC, C, P, and P+C groups. The lower the OD value, the weaker the proliferation ability of melanoma cells. C. Apoptosis ratio of melanoma cells in the NC and Apoptosis groups (n=12). D. Flow cytometric dot plot of apoptosis in NC group. E. Flow cytometric dot plot of apoptosis in Apoptosis group. F. The mRNA expression levels of FOXM1 between NC and Apoptosis groups. G. The OD value of melanoma cells in the NC and Apoptosis groups. H. The scratched area of melanoma cells at 0 h, 24 h, 48 h and 72 h. I. Proportion of scratched area of melanoma cells at 0 h, 24 h, 48 h and 72 h. *denotes *P* value < 0.05; **denotes *P* value < 0.01; ***denotes *P* value < 0.001; ****denotes *P* value < 0.0001.

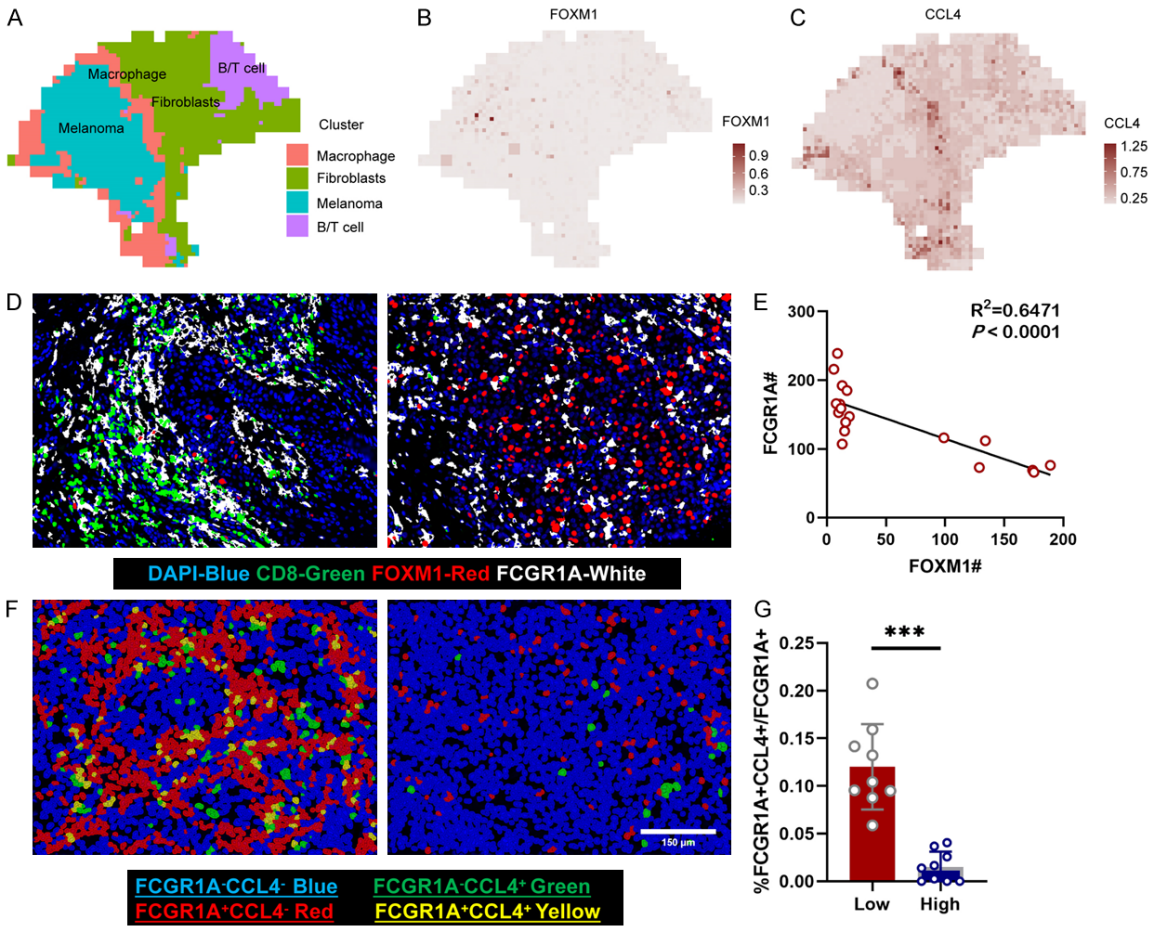

Figure 8. Expression of CCL4 and FOXM1 in spatial position information of melanoma samples. (A) In the spatial transcriptome analysis of melanoma sample, four kinds of cells (macrophages, fibroblasts, melanoma cells, and B/T cells) were annotated. (B) The signals of FOXM1was centered in the area of melanoma cells. (C) The CCL4 expression was centered on the macrophages. (D) Multi-immunohistochemistry staining in the skin paraffin sections from melanoma patients, Staining: CD8 (Green), FOXM1 (Red), FCGR1A (White); The melanoma sample with high FOXM1 expression (see right-hand of D) appeared much less tumor-infiltrating immune cells than the sample with low level of FOXM1 (see left-hand of D). (E) The correlation analysis between the counts of FOXM1 and the number of FCGR1A$^+$ macrophages in the same unit area. (F) Dual positive analysis results of multi-immunohistochemistry staining by inform analysis software. FCGR1A$^-$CCL4$^-$ cells were shown in Blue color; FCGR1A$^-$CCL4$^+$ cells were shown in Green color; FCGR1A$^+$CCL4$^-$ cells were shown in Red color; FCGR1A$^+$CCL4$^+$ cells were shown in Yellow color. The melanoma sample with high FOXM1 expression (see right-hand of F) appeared much less FCG1A$^+$CCL4$^+$ cells than the sample with low level of FOXM1 (see left-hand of F). (G) Based on the expression of FXOM1, melanoma samples were divided into FOXM1-high and FOXM1-low group. This figure showed that the percentage of FCGR1A$^+$CCL4$^+$ cells in the FOXM1-high group was significantly lower than that in the FOXM1-low group. *P* values were calculated with Student's t-test; ***denotes *P* value < 0.001.

expression of FOXM1 and decrease the proliferation and migration of melanoma cells.

We analyzed a previous melanoma spatial transcriptomics dataset to study the spatial information of CCL4 and FOXM1 in the tumor microenvironment [28]. The BayesSpace algorithm was used to improve the resolution of the dataset, and all spatial clusters were annotated into melanoma cells, fibroblasts, macrophages, and T/B cells based on biomarkers: PMEL, COL1A1, CD14, FCGR1A, CD19, and CD3D (**Figure 8A**, Supplementary Figure 3). FOXM1 appeared highly expressed in melanoma cells, while CCL4 showed a significant increase in macrophages surrounding the melanoma cells (**Figure 8B**, **8C**). The results of spatial transcriptome sequencing analysis also indicated that FOXM1 was closely associated with melanoma cells, whereas CCL4 was closely associated with macrophages, which would instruct us to follow up the study of the function of the two genes.

Meanwhile, we collected tissue sections of patients with melanoma for multiple immunohistochemistry staining. We found that samples with high FOXM1 expression had significantly reduced numbers of $CD8^+$ T cells and $FCGR1A^+$ macrophages (**Figure 8D**). The correlation between the FOXM1 intensity and the number of $FCGRA1^+$ cells in the same field of vision was analyzed, which showing a negative correlation between the FOXM1 and FCGR1A (**Figure 8E**). CCL4 was highly expressed in $FCGR1A^+$ macrophages. The melanoma samples with low FOXM1 intensity show significantly increased $CCL4^+FCGR1A^+$ cells than those with high FOXM1 intensity (**Figure 8F**, **8G**). These results suggested that CCL4 was highly expressed in macrophages surrounding melanoma cells and might influence the expression of FOXM1 in melanoma cells.

Discussion

Melanoma, known as the 'king of cancers', is a malignant tumor with high mortality, and metastasis rate, as well as great difficulty in treatment. There are nearly 20,000 new cases of melanoma in China each year, and the incidence rate is increasing year by year. With up to 3800 deaths per year, the mortality of melanoma in China accounts for 1/3 of all Asian patients and is ranked first in Asia [29]. Epidemiological data showed that the survival and treatment response rate of melanoma patients decreased as age increased [30]. Lung metastasis is the most common metastasis site for melanoma. 70% of patients with metastatic melanoma die for lung metastasis. Recent studies have shown that the lung microenvironment of aging individuals promotes dormant melanoma cells to transform into a proliferative active state, resulting in the formation of lung metastases [31]. Given the close relationship between melanoma and aging, we constructed a melanoma prognostic model based on aging-related genes CCL4 and FOXM1, in order to provide new ideas for melanoma risk prediction and prognosis evaluation.

When selecting variables that affect patient prognosis, we usually start by conducting univariate Cox analysis to screen for associated variables, and then build a multivariate model to further confirm whether the variables are independently associated with survival. However, when the number of variables is greater than the sample size, the traditional analysis methods of Cox regression are no longer applicable. Therefore, when the number of variables exceeds the sample size, one must first employ Lasso regression for variable selection, followed by the construction of a Cox regression model to analyze prognostic impact, which is the Lasso-Cox survival analysis model.

In this study, we found that FOXM1 and CCL4 are independent factors in the prognosis of melanoma patients using Lasso-Cox survival analysis model. Immune cell migration is well known to be necessary to initiate an effective anti-tumor immune response. $CD103^+$ DCs are thought to play a key role in helping effector T cells to migrate to tumor tissue areas and thus kill tumors [32]. The secretion of CCL4 has been confirmed to be essential in the recruitment of melanoma dermal $CD103^+$ DCs. The deficiency of CCL4 secretion function may result in reduced recruitment of $CD103^+$ DCs in the dermis, thus preventing the initiation of anti-tumor cell immune responses [33, 34]. Moreover, it has been shown that the CCL4-CCR5 axis-mediated migration of $CD8^+$ T cells is a determining factor in distinguishing immune-infiltrating tumors from immunosuppressive tumors [35].

As one key gene controlling cell proliferation, the abnormal activation of FOXM1 is closely associated with cancer cell proliferation and division. In normal keratinocytes, the expression of FOXM1 helps maintain keratinocytes high proliferative potential [36]. However, the abnormally high expression of FOXM1 has been demonstrated to be associated with poor clinical prognosis in multiple tumors. FOXM1 is critical to the genetic aberration and mutation required for the carcinogenesis of epidermal cells [37].

In this study, single-cell transcriptome analysis showed that FOXM1 was highly expressed in melanoma tumor cells, whereas CCL4 was significantly upregulated in tumor-infiltrating immune cells like T cells and macrophages. Further multiple immunohistochemical staining results revealed that the intensity of FOXM1 expression in the tumor region of melanoma was negatively correlated with the number of tumor-infiltrating immune cells. CCL4 was high-

ly expressed in macrophages surrounding tumor cells, consistent with the results from the spatial transcriptome. In addition, when FOXM1 expression was low in melanoma cells, CCL4 expression was increased in macrophages surrounding tumor cells, and there was a negative correlation between the two genes. Therefore, high expression of FOXM1 in tumor cells may indicate increased proliferation and division ability of cancer cells as well as stronger immune suppression, while there is a possible association between the higher CCL4 expression and more active tumor killing.

In the melanoma prognostic model constructed by the combination of FOXM1 and CCL4, the low-risk group appears more active immune response and weaker tumor proliferation ability, while the high-risk group may represent a stronger mitosis of cancer cells and less recruitment of anti-tumor immune cells. Hence, this model can well predict the 5-year survival rate of patients and the response rate to immune checkpoint therapy. The decrease in risk score for those melanoma patients after treatment further supports this speculation.

To further confirm the classification significance of this melanoma prognostic model, we used this model to divide melanoma patients into high-risk and low-risk groups, and compared the differences of gene mutation and transcription regulation between the two groups in detail. At the genetic level, cancer is essentially an abnormal and uncontrolled cell growth caused by genetic mutations. The driving of the oncogenic splicing switch in BCL2L12 can produce full-length BCL2L12, which gives cancer cells resistance to apoptosis and promotes tumor proliferation [38]. OGDH, as one of the glycolysis genes, can enhance mitochondrial function and activate the Wnt/β-catenin signaling pathway, thereby promoting tumor development [39]. When comparing gene mutations between high- and low-risk groups, we found that specific mutated genes such as BCL2L12 and OGDH were more common in the high-risk group. This suggests that our melanoma prognostic model can effectively screen patients who carry more driver oncogene mutations.

The dysregulation of DNA methylation is considered to play a major role in the inactivation of tumor suppressor genes or the abnormal activation of oncogenes in tumors. AMP-activated protein kinase (AMPK) is an important mediator for maintaining cellular energy homeostasis. It has been found that advanced cancer can trigger cellular recirculation signals of AMPK to phagocytose cellular debris and provide large tumors with the nutrients needed for growth [40]. MITF (Microphthalmia transcription factor) is a transcription factor that plays a key role in the occurrence and metastasis of malignant melanoma, and is also the most important direct oncogene in melanoma. High expression of MITF is often associated with highly malignant melanoma [41]. Previous studies have suggested that AMPK is an important regulator of MITF, and chemical inhibition of AMPK leads to a decrease in MITF protein levels [42]. In our melanoma prognostic model, the high-risk group showed high mRNA expression of AMPK signaling pathway-related genes as well as DNA hypomethylation, suggesting that aberrant activation of AMPK signaling pathway may play a key role in melanoma invasion progression as well as poor prognosis.

The miRNA, a class of small non-coding RNA molecules with regulatory functions, mainly regulate gene expression by inhibiting or breaking down target mRNAs at the translation level. As mentioned above, CCR5, as the receptor for CCL4, is expressed by various tumor-infiltrating immune cells. In our high-risk group of melanoma patients, CCR5 was lowly expressed, while the associated miRNA (miR211) was upregulated. Studies have shown that the expression of MIR211 in melanoma cell lines can lead to resistance to targeted therapy, which is consistent with the lower treatment response rate in our high-risk group [43].

The results of the multi-omics analysis showed that the molecular alterations in melanoma patients are complex, involving mutations, mRNA, methylation, and miRNA. Our analysis has revealed that that patients in the low-risk group perform better than those in the high-risk group in terms of mutations, mRNA, methylation, and miRNA, which may be the reason why patients in the low-risk group have better treatment outcomes and prognosis.

Conclusion

Our study establishes a melanoma prognostic model based on the aging-related genes, which

can be used to detect high-risk melanoma populations with poor prognosis and to predict immunotherapy response. In addition, population stratification based on this model can be used in tumor physiology studies of melanoma to investigate common characteristics of those melanoma patients with poor treatment prognosis, and thus provide ideas for subsequent clinical interventions and therapeutic targeting studies. Finally, we found that CCL4 was highly expressed in macrophages and might influence the expression of FOXM1 in melanoma cells through apoptosis.

Disclosure of conflict of interest

The authors declare that the research was conducted in the absence of any commercial or financial relationships that could be construed as a potential conflict of interest.

Abbreviations

TCGA, The Cancer Genome Atlas; GEO, Gene expression omnibus; DEGs, Differentially expressed genes; ROC, Receiver operating characteristic; AUC, Area under the ROC curve; GSEA, Gene set enrichment analysis; IHC, Immunohistochemistry; RT-qPCR, Quantitative real-time polymerase chain reaction; TIDE, Tumor immune dysfunction and exclusion; KEGG, Kyoto Encyclopedia of Genes and Genomes.

Address correspondence to: Zhijun Luo, Department of Plastic Surgery, Zhongshan City People's Hospital, Zhongshan, Guangdong, China. E-mail: hardaway2159@sina.com; Xidie Li, Department of Gynaecology and Obstetrics, The Affiliated Zhuzhou Hospital Xiangya Medical College, Central South University, Zhuzhou, Hunan, China. E-mail: lixidie1992@yeah.net

References

[1] Garg M, Couturier DL, Nsengimana J, Fonseca NA, Wongchenko M, Yan Y, Lauss M, Jönsson GB, Newton-Bishop J, Parkinson C, Middleton MR, Bishop DT, McDonald S, Stefanos N, Tadross J, Vergara IA, Lo S, Newell F, Wilmott JS, Thompson JF, Long GV, Scolyer RA, Corrie P, Adams DJ, Brazma A and Rabbie R. Tumour gene expression signature in primary melanoma predicts long-term outcomes. Nat Commun 2021; 12: 1137.

[2] Abu-Gheida I, Chao S, Murphy E, Suh J, Stevens GH, Mohammadi AM, McNamara M and Yu JS. Targeted therapy after brain radiotherapy for BRAF-mutated melanoma with extensive ependymal disease with prolonged survival: case report and review of the literature. Front Oncol 2019; 9: 168.

[3] Schadendorf D, van Akkooi ACJ, Berking C, Griewank KG, Gutzmer R, Hauschild A, Stang A, Roesch A and Ugurel S. Melanoma. Lancet 2018; 392: 971-984.

[4] Wohlmuth C and Wohlmuth-Wieser I. Vulvar melanoma: molecular characteristics, diagnosis, surgical management, and medical treatment. Am J Clin Dermatol 2021; 22: 639-651.

[5] Pye IM, Saw RPM and Saunderson RB. Vulvar melanoma. JAMA Dermatol 2023; 159: 96.

[6] Chattopadhyay C, Kim DW, Gombos DS, Oba J, Qin Y, Williams MD, Esmaeli B, Grimm EA, Wargo JA, Woodman SE and Patel SP. Uveal melanoma: from diagnosis to treatment and the science in between. Cancer 2016; 122: 2299-2312.

[7] Jung S and Johnson DB. Management of acral and mucosal melanoma: medical oncology perspective. Oncologist 2022; 27: 703-710.

[8] Broggi MAS, Maillat L, Clement CC, Bordry N, Corthésy P, Auger A, Matter M, Hamelin R, Potin L, Demurtas D, Romano E, Harari A, Speiser DE, Santambrogio L and Swartz MA. Tumor-associated factors are enriched in lymphatic exudate compared to plasma in metastatic melanoma patients. J Exp Med 2019; 216: 1091-1107.

[9] Ecker BL, Kaur A, Douglass SM, Webster MR, Almeida FV, Marino GE, Sinnamon AJ, Neuwirth MG, Alicea GM, Ndoye A, Fane M, Xu X, Sim MS, Deutsch GB, Faries MB, Karakousis GC and Weeraratna AT. Age-related changes in HAPLN1 increase lymphatic permeability and affect routes of melanoma metastasis. Cancer Discov 2019; 9: 82-95.

[10] Kaur A, Ecker BL, Douglass SM, Kugel CH 3rd, Webster MR, Almeida FV, Somasundaram R, Hayden J, Ban E, Ahmadzadeh H, Franco-Barraza J, Shah N, Mellis IA, Keeney F, Kossenkov A, Tang HY, Yin X, Liu Q, Xu X, Fane M, Brafford P, Herlyn M, Speicher DW, Wargo JA, Tetzlaff MT, Haydu LE, Raj A, Shenoy V, Cukierman E and Weeraratna AT. Remodeling of the collagen matrix in aging skin promotes melanoma metastasis and affects immune cell motility. Cancer Discov 2019; 9: 64-81.

[11] Jimenez F, Alam M, Vogel JE and Avram M. Hair transplantation: basic overview. J Am Acad Dermatol 2021; 85: 803-814.

[12] Goldman MJ, Craft B, Hastie M, Repečka K, McDade F, Kamath A, Banerjee A, Luo Y, Rogers D, Brooks AN, Zhu J and Haussler D. Visualizing and interpreting cancer genomics data via the Xena platform. Nat Biotechnol 2020; 38: 675-678.

[13] Jerby-Arnon L, Shah P, Cuoco MS, Rodman C, Su MJ, Melms JC, Leeson R, Kanodia A, Mei S, Lin JR, Wang S, Rabasha B, Liu D, Zhang G, Margolais C, Ashenberg O, Ott PA, Buchbinder EI, Haq R, Hodi FS, Boland GM, Sullivan RJ, Frederick DT, Miao B, Moll T, Flaherty KT, Herlyn M, Jenkins RW, Thummalapalli R, Kowalczyk MS, Cañadas I, Schilling B, Cartwright ANR, Luoma AM, Malu S, Hwu P, Bernatchez C, Forget MA, Barbie DA, Shalek AK, Tirosh I, Sorger PK, Wucherpfennig K, Van Allen EM, Schadendorf D, Johnson BE, Rotem A, Rozenblatt-Rosen O, Garraway LA, Yoon CH, Izar B and Regev A. A cancer cell program promotes T cell exclusion and resistance to checkpoint blockade. Cell 2018; 175: 984-997, e924.

[14] Zhao E, Stone MR, Ren X, Guenthoer J, Smythe KS, Pulliam T, Williams SR, Uytingco CR, Taylor SEB, Nghiem P, Bielas JH and Gottardo R. Spatial transcriptomics at subspot resolution with BayesSpace. Nat Biotechnol 2021; 39: 1375-1384.

[15] Bogunovic D, O'Neill DW, Belitskaya-Levy I, Vacic V, Yu YL, Adams S, Darvishian F, Berman R, Shapiro R, Pavlick AC, Lonardi S, Zavadil J, Osman I and Bhardwaj N. Immune profile and mitotic index of metastatic melanoma lesions enhance clinical staging in predicting patient survival. Proc Natl Acad Sci U S A 2009; 106: 20429-20434.

[16] Cabrita R, Lauss M, Sanna A, Donia M, Skaarup Larsen M, Mitra S, Johansson I, Phung B, Harbst K, Vallon-Christersson J, van Schoiack A, Lövgren K, Warren S, Jirström K, Olsson H, Pietras K, Ingvar C, Isaksson K, Schadendorf D, Schmidt H, Bastholt L, Carneiro A, Wargo JA, Svane IM and Jönsson G. Tertiary lymphoid structures improve immunotherapy and survival in melanoma. Nature 2020; 577: 561-565.

[17] Mayakonda A, Lin DC, Assenov Y, Plass C and Koeffler HP. Maftools: efficient and comprehensive analysis of somatic variants in cancer. Genome Res 2018; 28: 1747-1756.

[18] Ritchie ME, Phipson B, Wu D, Hu Y, Law CW, Shi W and Smyth GK. Limma powers differential expression analyses for RNA-sequencing and microarray studies. Nucleic Acids Res 2015; 43: e47.

[19] Robinson MD, McCarthy DJ and Smyth GK. edgeR: a Bioconductor package for differential expression analysis of digital gene expression data. Bioinformatics 2010; 26: 139-140.

[20] Sticht C, De La Torre C, Parveen A and Gretz N. miRWalk: an online resource for prediction of microRNA binding sites. PLoS One 2018; 13: e0206239.

[21] Tian Y, Morris TJ, Webster AP, Yang Z, Beck S, Feber A and Teschendorff AE. ChAMP: updated methylation analysis pipeline for Illumina BeadChips. Bioinformatics 2017; 33: 3982-3984.

[22] Yu G, Wang LG, Han Y and He QY. clusterProfiler: an R package for comparing biological themes among gene clusters. OMICS 2012; 16: 284-287.

[23] Yoshihara K, Shahmoradgoli M, Martínez E, Vegesna R, Kim H, Torres-Garcia W, Treviño V, Shen H, Laird PW, Levine DA, Carter SL, Getz G, Stemke-Hale K, Mills GB and Verhaak RG. Inferring tumour purity and stromal and immune cell admixture from expression data. Nat Commun 2013; 4: 2612.

[24] Newman AM, Liu CL, Green MR, Gentles AJ, Feng W, Xu Y, Hoang CD, Diehn M and Alizadeh AA. Robust enumeration of cell subsets from tissue expression profiles. Nat Methods 2015; 12: 453-457.

[25] Fu J, Li K, Zhang W, Wan C, Zhang J, Jiang P and Liu XS. Large-scale public data reuse to model immunotherapy response and resistance. Genome Med 2020; 12: 21.

[26] Bagaev A, Kotlov N, Nomie K, Svekolkin V, Gafurov A, Isaeva O, Osokin N, Kozlov I, Frenkel F, Gancharova O, Almog N, Tsiper M, Ataullakhanov R and Fowler N. Conserved pan-cancer microenvironment subtypes predict response to immunotherapy. Cancer Cell 2021; 39: 845-865, e847.

[27] Liao YH, Hsu SM and Huang PH. ARMS depletion facilitates UV irradiation induced apoptotic cell death in melanoma. Cancer Res 2007; 67: 11547-11556.

[28] Thrane K, Eriksson H, Maaskola J, Hansson J and Lundeberg J. Spatially resolved transcriptomics enables dissection of genetic heterogeneity in stage III cutaneous malignant melanoma. Cancer Res 2018; 78: 5970-5979.

[29] National Health Commission of the People's Republic of China. Chinese Protocol of Diagnosis and Treatment of Colorectal Cancer (2020 edition). Zhonghua Wai Ke Za Zhi 2020; 58: 561-585.

[30] Ribero S, Stucci LS, Marra E, Marconcini R, Spagnolo F, Orgiano L, Picasso V, Queirolo P, Palmieri G, Quaglino P and Bataille V. Effect of age on melanoma risk, prognosis and treatment response. Acta Derm Venereol 2018; 98: 624-629.

[31] Fane ME, Chhabra Y, Alicea GM, Maranto DA, Douglass SM, Webster MR, Rebecca VW, Marino GE, Almeida F, Ecker BL, Zabransky DJ, Hüser L, Beer T, Tang HY, Kossenkov A, Herlyn M, Speicher DW, Xu W, Xu X, Jaffee EM, Aguirre-Ghiso JA and Weeraratna AT. Stromal changes in the aged lung induce an emergence from melanoma dormancy. Nature 2022; 606: 396-405.

[32] Hiam-Galvez KJ, Allen BM and Spitzer MH. Systemic immunity in cancer. Nat Rev Cancer 2021; 21: 345-359.
[33] Spranger S and Gajewski TF. Tumor-intrinsic oncogene pathways mediating immune avoidance. Oncoimmunology 2015; 5: e1086862.
[34] Pai SG, Carneiro BA, Mota JM, Costa R, Leite CA, Barroso-Sousa R, Kaplan JB, Chae YK and Giles FJ. Wnt/beta-catenin pathway: modulating anticancer immune response. J Hematol Oncol 2017; 10: 101.
[35] Reschke R and Gajewski TF. CXCL9 and CXCL10 bring the heat to tumors. Sci Immunol 2022; 7: eabq6509.
[36] Smirnov A, Panatta E, Lena A, Castiglia D, Di Daniele N, Melino G and Candi E. FOXM1 regulates proliferation, senescence and oxidative stress in keratinocytes and cancer cells. Aging (Albany NY) 2016; 8: 1384-1397.
[37] Teh MT, Gemenetzidis E, Chaplin T, Young BD and Philpott MP. Upregulation of FOXM1 induces genomic instability in human epidermal keratinocytes. Mol Cancer 2010; 9: 45.
[38] Wang Z, Wang S, Qin J, Zhang X, Lu G, Liu H, Guo H, Wu L, Shender VO, Shao C, Kong B and Liu Z. Splicing factor BUD31 promotes ovarian cancer progression through sustaining the expression of anti-apoptotic BCL2L12. Nat Commun 2022; 13: 6246.
[39] Lu X, Wu N, Yang W, Sun J, Yan K and Wu J. OGDH promotes the progression of gastric cancer by regulating mitochondrial bioenergetics and Wnt/β-catenin signal pathway. Onco Targets Ther 2019; 12: 7489-7500.
[40] Eichner LJ, Brun SN, Herzig S, Young NP, Curtis SD, Shackelford DB, Shokhirev MN, Leblanc M, Vera LI, Hutchins A, Ross DS, Shaw RJ and Svensson RU. Genetic analysis reveals AMPK is required to support tumor growth in murine Kras-dependent lung cancer models. Cell Metab 2019; 29: 285-302, e287.
[41] Liu Z, Chen K, Dai J, Xu P, Sun W, Liu W, Zhao Z, Bennett SP, Li P, Ma T, Lin Y, Kawakami A, Yu J, Wang F, Wang C, Li M, Chase P, Hodder P, Spicer TP, Scampavia L, Cao C, Pan L, Dong J, Chen Y, Yu B, Guo M, Fang P, Fisher DE and Wang J. A unique hyperdynamic dimer interface permits small molecule perturbation of the melanoma oncoprotein MITF for melanoma therapy. Cell Res 2023; 33: 55-70.
[42] Borgdorff V, Rix U, Winter GE, Gridling M, Müller AC, Breitwieser FP, Wagner C, Colinge J, Bennett KL, Superti-Furga G and Wagner SN. A chemical biology approach identifies AMPK as a modulator of melanoma oncogene MITF. Oncogene 2014; 33: 2531-2539.
[43] Sahoo A, Sahoo SK, Joshi P, Lee B and Perera RJ. MicroRNA-211 loss promotes metabolic vulnerability and BRAF inhibitor sensitivity in melanoma. J Invest Dermatol 2019; 139: 167-176.

Supplementary Table 1. Prognostic related genes in patients with melanoma

Gene	coef	se	z	p
BIRC3	0.661	0.145	4.558	0
C1QA	0.539	0.144	3.749	0
CCL4	0.614	0.143	4.295	0
DDX58	0.557	0.142	3.925	0
DLL3	-0.5	0.143	-3.488	0
FBP1	0.564	0.143	3.952	0
FGF7	0.62	0.144	4.316	0
FOXM1	-0.537	0.143	-3.752	0
IL15	0.566	0.144	3.921	0
IL7R	0.557	0.144	3.858	0
JAK2	0.569	0.147	3.88	0
RELB	0.527	0.143	3.694	0
SOD2	0.643	0.143	4.49	0
SSTR3	0.5	0.142	3.523	0
STAT3	0.515	0.142	3.632	0
TLR4	0.523	0.144	3.629	0
TNFRSF11B	0.544	0.143	3.814	0
TNFSF13B	0.529	0.146	3.615	0
TRAF1	0.579	0.142	4.072	0
VCAM1	0.599	0.147	4.071	0
AXL	0.497	0.144	3.458	0.001
CBX7	0.445	0.14	3.178	0.001
CCL13	0.466	0.141	3.311	0.001
CCL7	0.459	0.141	3.263	0.001
CSF2RB	0.477	0.142	3.354	0.001
ESR1	0.482	0.141	3.417	0.001
HK3	0.473	0.142	3.328	0.001
HRAS	-0.473	0.144	-3.283	0.001
IL2RB	0.464	0.142	3.262	0.001
KCNA3	0.496	0.144	3.437	0.001
PTK2B	0.478	0.141	3.386	0.001
TIMP1	0.464	0.142	3.268	0.001
TNF	0.495	0.143	3.455	0.001
IL2RG	0.444	0.143	3.096	0.002
IL7	0.443	0.141	3.131	0.002
MAP3K5	0.44	0.144	3.062	0.002
MYD88	0.445	0.141	3.149	0.002
PIK3R2	-0.429	0.141	-3.044	0.002
PRKACB	0.44	0.145	3.034	0.002
TGFB1	0.427	0.141	3.036	0.002

Supplementary Table 2. The codes for screening key genes

```
rm(list=ls())
options(stringsAsFactors = F)
load(file = "step1output.Rdata")
mm=read.csv(file = 'genes.txt',sep = '\t',header = T)
gene=mm$Symbol
exprSet=exprSet[gene,]
exprSet=na.omit(exprSet)
table(rowSums(exprSet==0)==ncol(exprSet))
exprSet=exprSet[which(apply(exprSet,1,function(x){return(sum(x>0.00001))})>ncol(exprSet)*0.5),]
exprSet <- exprSet[apply(exprSet,1,sum)!=0,]
gene=rownames(exprSet)
a=read.csv(file = 'fsam.txt',sep = '\t')
sam=a$sam
b=exprSet[,sam]
group_list=ifelse(as.numeric(substr(colnames(b),14,15)) < 10,'tumor','normal')
table(group_list)
meta=read.csv(file = 'mete.txt',sep = '\t')
library(survival)
library(survminer)
dim(expr)
dim(meta)
exprSet=na.omit(b)
head(meta)
colnames(meta)
meta[,3][is.na(meta[,3])]=0
meta[,4][is.na(meta[,4])]=0
meta$days=as.numeric(meta[,3])+as.numeric(meta[,4])
meta=meta[,c(1:2,5:8,12)]
colnames(meta)=c('ID','event','race','age','gender','stage',"days")
meta$event=ifelse(meta$event=='Alive',0,1)
meta$age=as.numeric(meta$age)
library(stringr)
meta$stage=str_split(meta$stage,' ',simplify = T)[,2]
table(   meta$stage)
boxplot(meta$age)
meta$age_group=ifelse(meta$age>median(meta$age),'older','younger')
table(meta$race)
meta$time=meta$days/30
phe=meta
phe$ID=toupper(phe$ID)
phe=phe[match(substr(colnames(exprSet),1,12),phe$ID),]
colnames(phe)
phe=na.omit(phe)
exprSet=exprSet[,substr(colnames(exprSet),1,12) %in% phe$ID]
z=colnames(exprSet)
phe$ID=z
mySurv=with(phe,Surv(time, event))
cox_results <-apply(exprSet , 1 , function(gene){
   group=ifelse(gene>median(gene),'high','low')
   survival_dat <- data.frame(group=group,stage=phe$stage,age=phe$age,
                                        stringsAsFactors = F)
m=coxph(mySurv ~ age + stage+ group, data =  survival_dat)
```

```
beta <- coef(m)
se <- sqrt(diag(vcov(m)))
HR <- exp(beta)
HRse <- HR * se
tmp <- round(cbind(coef = beta, se = se, z = beta/se, p = 1 - pchisq((beta/se)^2, 1),
                                HR = HR, HRse = HRse,
                                HRz = (HR - 1) / HRse, HRp = 1 - pchisq(((HR - 1)/HRse)^2, 1),
                                HRCILL = exp(beta - qnorm(.975, 0, 1) * se),
                                HRCIUL = exp(beta + qnorm(.975, 0, 1) * se)), 3)
  return(tmp['grouplow',])

})
cox_results=t(cox_results)
table(cox_results[,4]<0.05)
cox_results[cox_results[,4]<0.05,]
cox=cox_results[cox_results[,4]<0.05,]

gene=rownames(cox)
e=t(exprSet[gene,])
dat=cbind(phe,e)
dat$gender=factor(dat$gender)
dat$stage=factor(dat$stage)
colnames(dat)

library(lars)
library(glmnet)
exprSet=exprSet[gene,]
x=t(exprSet)
y=phe$event

model_lasso <- glmnet(x, y, family="binomial", nlambda=50, alpha=1)
print(model_lasso)
head(coef(model_lasso, s=c(model_lasso$lambda[29],0.009)))
plot(model_lasso, xvar = "norm", label = TRUE)
plot(model_lasso, xvar="lambda", label=TRUE)
cv_fit <- cv.glmnet(x=x, y=y, alpha = 1, nlambda = 1000)
plot(cv_fit)
c(cv_fit$lambda.min,cv_fit$lambda.1se)
model_lasso <- glmnet(x=x, y=y, alpha = 1, lambda=cv_fit$lambda.1se)
lasso.prob <- predict(cv_fit, newx=x , s=c(cv_fit$lambda.min,cv_fit$lambda.1se) )
re=cbind(y ,lasso.prob)
dat=as.data.frame(re[,1:2])
colnames(dat)=c('event','prob')
dat$event=as.factor(dat$event)
library(ggpubr)
p <- ggboxplot(dat, x = "event", y = "prob",
                        color = "event", palette = "jco",
                        add = "jitter")
p + stat_compare_means()
library(ROCR)
library(glmnet)
library(caret)
pred <- prediction(re[,2], re[,1])
perf <- performance(pred,"tpr","fpr")
```

```
performance(pred,“auc”)
plot(perf,colorize=FALSE, col=“black”)
lines(c(0,1),c(0,1),col = “gray”, lty = 4 )
fit <- glmnet(x=x, y=y, alpha = 1, lambda=cv_fit$lambda.1se)
head(fit$beta)
choose_gene=rownames(fit$beta)[as.numeric(fit$beta)!=0]
length(choose_gene)
myexpr=x[,choose_gene]
mysurv=phe[,c(“days”,“event”)]
mysurv$days[mysurv$days< 1] = 1
fit <- glmnet( myexpr, Surv(mysurv$days,mysurv$event),
                        family = “cox”)
plot(fit, xvar=“lambda”, label = TRUE)
plot(fit, label = TRUE)

e=t(exprSet[c(‘CCL4’,‘FOXM1’),])
dat=cbind(phe,e)
dat$gender=factor(dat$gender)
dat$stage=factor(dat$stage)

colnames(dat)
s=Surv(time, event) ~ CCL4+FOXM1
model <- coxph(s, data = dat )
summary(model,data=dat)
options(scipen=1)
ggforest(model, data =dat,
               main = “Hazard ratio”,
               cpositions = c(0.10, 0.22, 0.4),
               fontsize = 1.0,
               refLabel = “1”, noDigits = 4)

fp <- predict(model)
summary(model,data=dat)
library(Hmisc)
options(scipen=200)
with(dat,rcorr.cens(fp,Surv(time, event)  ))

phe=dat[,c(1:2,4,9,10,11)]

gs=c(‘FOXM1’)
splots <- lapply(gs, function(g){
   phe$gene=ifelse(phe[,g]>quantile(phe[,g],probs = 0.5),‘high’,‘low’)
   sfit1=survfit(Surv(time, event)~gene, data=phe)
   ggsurvplot(sfit1,pval =TRUE, data = phe)
})
p=arrange_ggsurvplots(splots, print = TRUE,ncol = 1, nrow = 1, risk.table.height = 0.4)
```

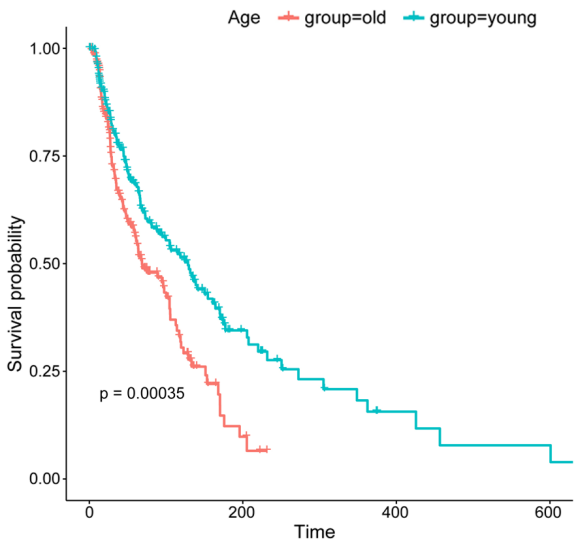

Supplementary Figure 1. Melanoma patients were grouped by age and survival analysis revealed that older patients had worse prognosis.

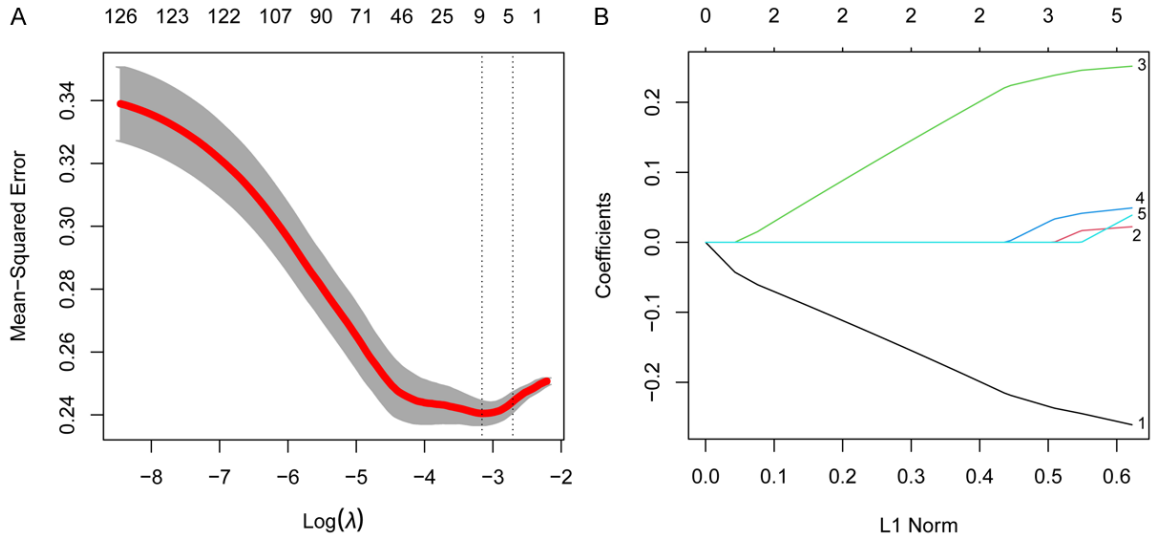

Supplementary Figure 2. Lasso analysis of senescence genes associated with prognosis obtained from cox analysis was performed to further narrow the scope of key genes.

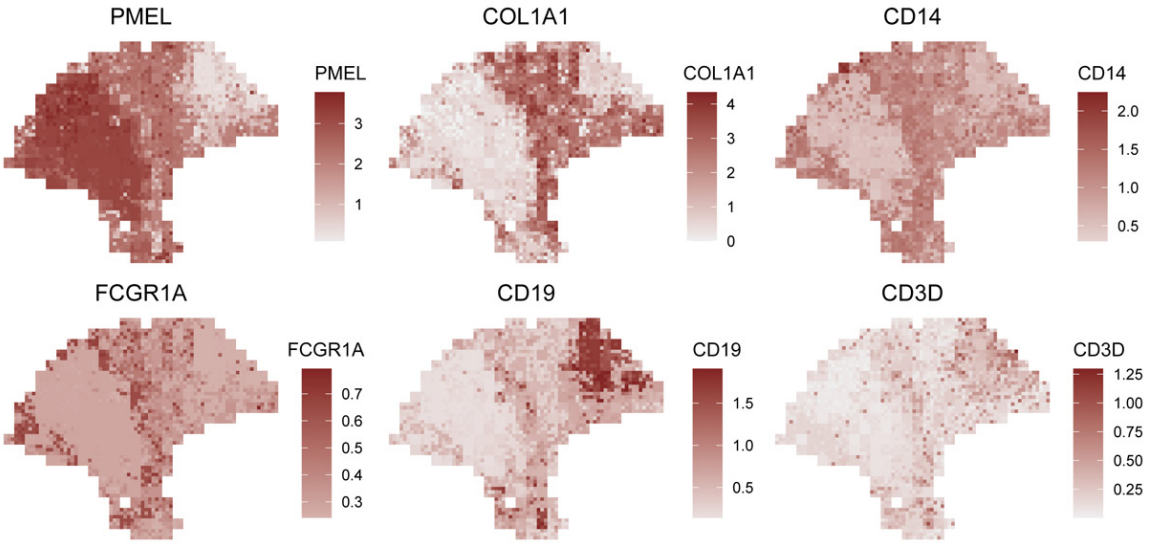

Supplementary Figure 3. Expression levels of PMEL, COL1A1, CD14, FCGR1A, CD19, and CD3D in the transcriptome of melanoma.